INTERNATIONAL JOURNAL FOR NUMERICAL METHODS IN FLUIDS, VOL. 1, 101–115 (1981)

SUBSIDENCE ABOVE VOLUMETRIC AND WATERDRIVE GAS RESERVOIRS

B. A. SCHREFLER

Department of Civil Engineering, University of Padua, Padua, Italy

R. W. LEWIS

Department of Civil Engineering, University of Wales, Swansea, U.K.

AND

C. MAJORANA

Department of Civil Engineering, University of Padua, Padua, Italy

SUMMARY

A fully coupled consolidation model has been developed for the simulation of the surface subsidence above gas reservoirs. The model is based on the Biot Theory and the material balance equation for hydrocarbon reservoirs. The model is extremely versatile and can handle such complex situations as vertical cross-sections where several gas reservoirs and aquifers are exploited at different levels. Computer runs were used to generate several reservoir formation profiles and the surface subsidence bowl for a variety of conditions. These results indicate the importance of various parameters which are disregarded in proelasticity models.

KEY WORDS Subsidence Finite Elements Reservoirs Hydrocarbons Pore Pressure Consolidation Aquifer Waterdrive Permeability

INTRODUCTION

The production of hydrocarbons from subsurface reservoirs is often accompanied by settlements at the ground surface, caused by a pressure reduction in the fluids within the reservoir rocks. These settlements are of great concern if heavy populated areas are involved. Long Beach (California), Groningen (Holland) and now also Ravenna (Italy) are well-known examples. In this latter case subsurface gas reservoirs both onshore and offshore are exploited and the resulting settlements may modify permanently the existing shoreline.

Two main types of numerical models are currently used for the prediction of man-induced settlements above surface hydrocarbon reservoirs. The first type investigates the subsidence in terms of reservoir compaction only. In this case the effects of an isolated volume of reduced pore pressure in a porous or nonporous, linearly elastic halfspace are studied. The interaction between the shrinking inclusion and the surroundings is calculated using the

0271-2091/81/020101-15$01.50 *Received 19 September 1980*

theory of poroelasticity[1,2] and the nucleus-of-strain concept. Usually both the reservoir and its surroundings are treated as homogeneous materials. In the theory of poroelasticity the reservoir is assumed to be separated from the surrounding halfspace by an impermeable barrier. No exchange of fluid between the reservoir layers and the limiting strata can take place. A consequence of this assumption is that the consolidation of surrounding clays is disregarded. It has been shown in Reference 3 that the contribution of limiting clay layers to the subsidence can be equivalent to that of the reservoir compaction itself. Many productive zones show the presence of clay as for instance in the Goose Creek field, Lake Maracaibo reservoir, Bachaquero reservoir and the Ravenna field.

Also the encroaching edge or bottom water, often present in reservoirs, is only taken into account for the determination of the varying reservoir pressure.[4] The influence of its flow upon consolidation is disregarded. It will be shown in this paper that the flow of edge water penetrating in the reservoir produces an increase of the areal extent of the surface settlement.

An improved version of the poroelasticity model has been presented by Finol and Farouq Ali.[5] The authors obtain the local compaction distribution in a reservoir by means of a reservoir simulator. The compaction is then related to the subsidence occurring at the surface by means of a poroelastic analysis.

The second type of model has been developed by two of the present authors.[3,6,7] It makes use of a fully coupled finite element consolidation program based on the Biot theory and of the material balance equation for the hydrocarbon pool only. It has all the advantages of the usual finite element models in soil mechanics, i.e. it is easily applicable to real stratigraphies, admits several source points or pools and takes into account linear and nonlinear elastic and elastoplastic constitutive relationships. This latter point is important for the simulation of the subsidence after the shutdown of the production wells, when the pressure in the pool increases again due to encroaching edge or bottom water.

The present model with the material balance equation applies to reservoirs of limited lateral extension when compared to the depth of burial. A typical case of this kind is the Ravenna field,[8] where the productive zone covers seven stacked intervals distributed over a vertical section from 1270 m to 2048 m below the surface. The most important pool of this field is located between 1678 m and 1803 m, has a formation thickness of maximum 65 m and covers an area of 15·6 km^2. The porosity of the reservoir sand is 26·6 per cent, the mean value of the permeability 168 md, the temperature 38°C and the initial pressure 19·7 MPa.

An alternative method, which applies also to extended reservoirs with a small depth of burial is currently under investigation.[9] This method consists of taking a vertical cross-section of the rock structure and performing a stress analysis on both the reservoir and the overburden assuming no flow to have taken place. The finite element method is used for the space discretization of this problem to arrive at an initial stress field throughout the section. The fluids are assumed to flow in a bounded subregion with the water displacing the gas or oil and the simultaneous flow of these fluids is also analysed by the finite element method. From the combined analysis an effective stress field is evaluated throughout the region as a function of time and used to evaluate the displacements at any given time.

The aim of the present paper is to investigate with the consolidation model a nonhomogeneous vertical cross section with a waterdrive and a volumetric gas reservoir. The influence of several material and geometric parameters upon the surface settlement is shown. This indicates the importance of those parameters which are disregarded in the poroelasticity models.

THE FINITE ELEMENT MODEL

The three-dimensional consolidation process, taking into account the compressibility of the fluid and of the solid particles,[6] is governed by the following coupled equations:

Equilibrium equations

$$[D_{ijkl}\dot{u}_{(k,l)}]_{,i} + \delta_{ij}\dot{p}_{,i} - \left(D_{ijkl}\delta_{kl}\frac{\dot{p}}{3k_s}\right)_{,i} + \rho F_i = 0 \tag{1}$$

Continuity equations

$$[k_{ij}(p_{,j} + \rho_2 F_j)]_{,i} + \dot{u}_{i,i} - \frac{1}{3k_s}\delta_{ij}D_{ijkl}\dot{u}_{(k,l)} - \frac{\dot{p}}{k_f} + \frac{1}{(3k_s)^2}\delta_{ij}D_{ijkl}\delta_{kl}\dot{p} = 0 \tag{2}$$

where u_i, F_j, D_{ijkl}, k_{ij} denote the Cartesian components, respectively, of the displacement vector, the body force vector, the effective stress tangent modulus tensor ($D_{ijkl} = D_{jikl} = D_{ijlk} = D_{klij}$) and the permeability tensor; p denotes the pre-water pressure, ρ the mass density of the saturated soil and ρ_2 the mass density of the pore fluid. k_s denotes the bulk modulus of soil grains and k_f denotes the combined compressibility of the fluid and the solid δ_{ij} is the Kronecker delta. A superposed dot indicates differentiation with respect to the time variable.

The associated boundary conditions are of the following four types: prescribed displacements $\bar{u}_i$, prescribed tractions $\bar{T}$, prescribed pore pressures $\bar{p}$, prescribed flow (normal to the boundary) $\bar{Q}_i$.

In addition to equations (1) and (2), the material balance equation for the gas has to be included for the gas reservoir[3] viz:

$$GB_{gi} = (G - G_p)B_g + W_e - B_w W_p \tag{3}$$

where

G = gas initially contained in the reservoir
G_p = gas production
B_g = formation volume factor for gas
W_e = water influx from the adjacent aquifer
B_w = formation volume factor for water
W_p = water production

This equation is essentially a volumetric balance at reservoir condition for the fluids contained initially in the gas reservoir, the portion of these fluids still remaining at a later date, plus the encroaching water from the adjacent aquifer and the water drained from the bounding strata.

The material-blance equation is applicable only to the reservoir as a whole because of the migration of gas from one position to another.

The formation volume factor relates the volume of gas within the reservoir to the volume at standard conditions on the surface, i.e.

$$B_g = \frac{P_{sc}}{T_{sc}}\frac{ZT}{P}$$

where $Z(P, T)$ is the compressibility factor.

The technique chosen for the transient solution of the simultaneous nonlinear equations is a single step iterative method. For a typical time-step the logic of the scheme is as follows:

1. At time t the water influx into the reservoir, the cumulative gas production, the reservoir conditions and the water and gas production for the time step Δt are all known. Using an iterative procedure, the material balance equation yields the resulting mean value of the pore pressure in the reservoir,

$$\frac{P}{Z(P,T)} = \frac{(G-G_p)T}{GZ(P_i,T_i)\frac{T_i}{P_i} - \frac{T_{sc}}{P_{sc}}(W_e - B_w W_p)}$$

2. Apply the resulting variation in pressure of the reservoir to the coupled equations (1) and (2), and calculate $\Delta\bar{u}$ and Δp and the new water influx in the reservoir for the next time step.

The procedure adopted for the solution of the three simultaneous nonlinear equations needs some comment. A straightforward application of the outlined procedure means,

(a) that the variation of the equivalent bulk modulus of the pore fluid due to the upward displacement of the gas–water contact surface is neglected as well as,
(b) the change from actual weight to submerged weight for the same reason.

A better approximation can be obtained by updating these material properties for the reservoir elements when the water–gas contact surface moves through the same elements. An approximated instantaneous position of the contact surface can be obtained from the total water influx, the porosity and reservoir volume.

The form of material balance equation used neglects some minor factors such as the variation in volume of the interstitial water with pressure, the change of porosity with pressure and the evolution of gas dissolved in the interstitial water with decrease in pressure. These factors may be included in the material balance where warranted by the precision of available data.

The use of a generalized material balance equation,[10]

$$N(B_{t_i} - B_t) + N_p[B_t + (R_p - R_{s_i})B_g] + NmB_{t_i}\left(1 - \frac{B_g}{B_{g_i}}\right) = W_e - B_w W_p$$

allows an extension of the proposed method for investigation of surface subsidence in gas-condensate reservoirs, under-saturated oil reservoirs and oil reservoirs with simultaneous drives such as dissolved gas drive, gas cap drive and water drive within the framework of the approximations already mentioned.

CONSTITUTIVE RELATIONSHIPS

Various constitutive relationships are currently in use for the solution of soil consolidation problems. These consist of linear elastic, nonlinear and elastoplastic relationships.

The nonlinear stress/strain rule is that suggested by Duncan and Chang,[11] which uses the hyperbolic equation

$$(\sigma_1 - \sigma_3) = \frac{\varepsilon}{a + b\varepsilon}$$

where σ_1 and σ_3 are the major and minor principal stresses, ε is the strain in the σ_1-direction and a and b are experimentally determined constants. Also, the initial tangent modulus, E_i,

is assumed to be given by

$$E_i = KP_a\left(\frac{\sigma_3}{P_a}\right)^n$$

where P_a = atmospheric pressure and K and n are constants determined from a set of triaxial tests.

For the elastoplastic model the yield criteria are given by a nonassociated Mohr–Coulomb surface and a critical state ellipse. A modified form of the latter is dependent on the third stress invariant such that a cross-section perpendicular to the mean stress or J_1-axis has the same shape as the Mohr–Coulomb yield surface, i.e. the slope of the critical state line is given by a Mohr–Coulomb line for which the cohesion intercept is zero. A further variation of the critical state model uses the critical state elliptical yield surface only for stress states below the critical state line, whilst using a Mohr–Coulomb yield surface for states above this line.

PARAMETRIC INVESTIGATIONS

A hypothetical axisymmetric cross-section with a gas reservoir at 1800 m below surface has been studied. The reservoir thickness varies between 80 m and 40 m and the radius between 1000 m and 2000 m. In the case of a waterdrive reservoir an adjacent aquifer has been assumed with the same thickness as the reservoir itself. Both the reservoir and the aquifer are overlain by a clay layer of 80 m thickness. The volume reservoir is overlain and laterally bounded by clay. The remaining depth of the vertical cross-section is assumed to be of sand.

The initial reservoir pressure is 19·7 MPa, the gas contained initially in the pool is 13×10^9 Nm^3.[4] The temperature in the pool is 40°C. The time of exploitation of the reservoir has been assumed to be 10 years with the cumulative gas production versus time shown in Figure 1. The production from the reservoir is supposed to be effected through several wells

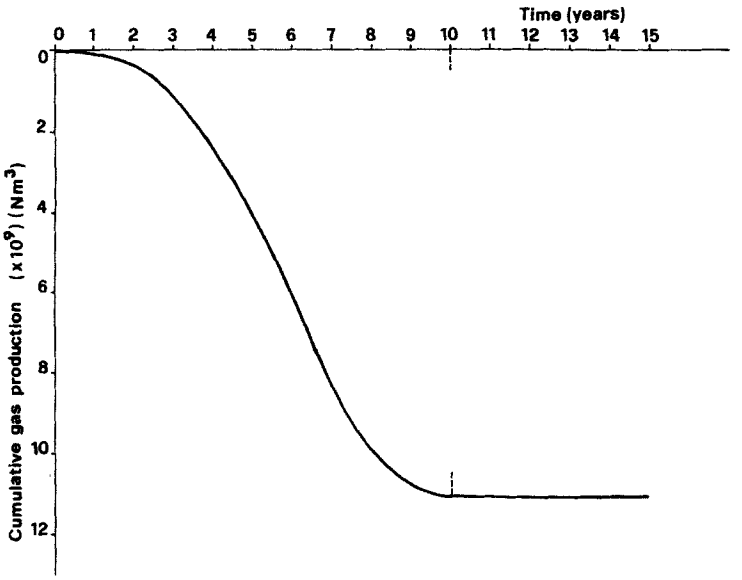

Figure 1. Production history assumed for the simulations

producing at the same rate and evenly spaced in the reservoir. This generates a reasonably uniform pressure drop over the whole reservoir.

The modulus of elasticity for the sand is $E = 9{\cdot}9$ MPa,[6] and that for the clay, which bounds the reservoir, is $E = 3{\cdot}92$ MPa. Poisson's ratio is 0·20 for the sand and 0·45 for the clay. The permeability of the clay has been assumed to be $8{\cdot}65 \times 10^{-5}$ m/day, for the sand on the top of the model 4·32 m/day and for the reservoir and the limiting aquifer in turn 0·0471, 0·7358 and 1·8396 m/day (respectively 12·8, 200 and 500 md). For comparison the permeabilities in the Ravenna field vary between 10 and 776 md. More in general, the assumed values for the geometrical parameters, temperature, initial pressure are within the range of those observed in the Ravenna field, while the material properties have been obtained from a deep borehole in Venice. Both areas have a similar geological history and physical environment.

RESULTS

A graph of subsidence versus time for a waterdrive reservoir with different values of the reservoir permeability is plotted in Figure 2. The increase of the permeability reduces the maximum observed subsidence because the major quantity of penetrating edge water reduces the drop of the reservoir pressure. When the permeability increases, the peak value of subsidence is reached earlier. The radial extension of the resulting subsidence bowl increases with the permeability because the flow in the aquifer affects zones with greater radial distance.

The settlement versus time at the centre of the model and at three different levels is shown in Figure 3 for the case of a waterdrive reservoir with an outer reservoir radius $R_w = 1000$ m

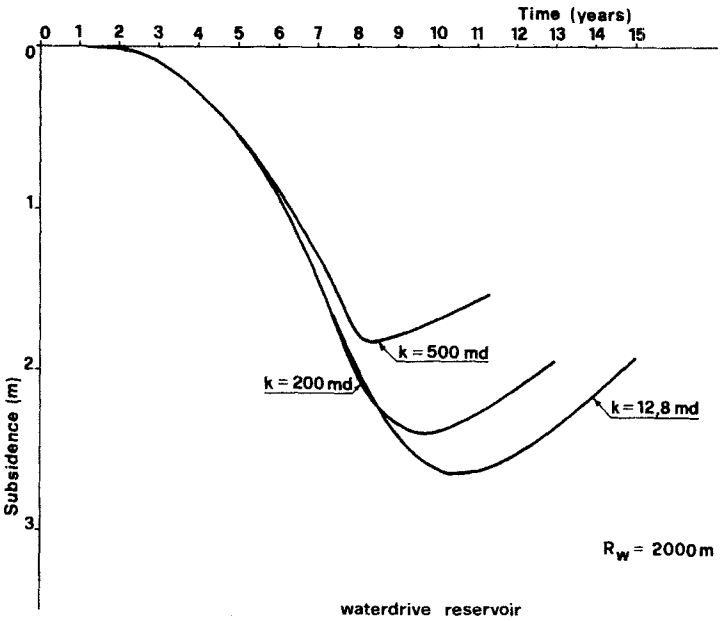

Figure 2. Waterdrive reservoir: substance versus time for different values of the reservoir permeability

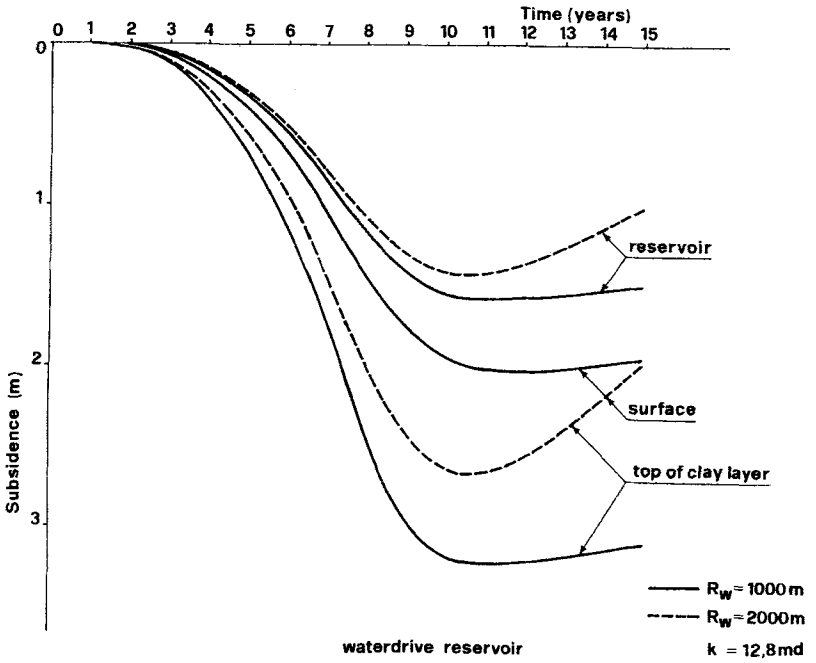

Figure 3. Waterdrive reservoir: settlement in time for two values of the reservoir radius

and 2000 m. The permeability of the reservoir and aquifer is 12·8 md. It can be seen that in both cases the reservoir compaction is considerably smaller than the settlement observed at the surface. The compaction of the clay layer in the case of $R_w = 1000$ m is larger than for $R_w = 2000$ m, in accordance with the higher drop in reservoir pressure shown in Figure 4. In the case of $R_w = 1000$ m the sand layer on the top of the model is slightly expanding. The recovery of the deformation after the end of exploitation is faster for $R_w = 2000$ m. This fact is consistent with the higher water inflow shown in Figure 5. It is interesting to note that the water inflow versus time plots are similar in both cases.

The same quantities as in Figure 3 are shown in Figure 6 for a volumetric reservoir. Again the reservoir compaction and the settlement at the top of the clay layer is bigger in the case of $R_w = 1000$ m than for $R_w = 2000$ m. This is in accordance with the larger drop of the reservoir pressure for $R_w = 1000$ m, shown in Figure 7. This time the expansion of the huge sand layer on the top of the limiting clay layers can be observed in both cases.

Comparing the diagrams for $R_w = 2000$ m in Figures 3 and 6 it can be seen that the maximum compactions of the reservoir and the clay layer are very close but that the recovery after the abandonment is obviously quicker in the case of a waterdrive reservoir. This can be explained by the fact that even in a volumetric reservoir bounded by clay a not inconsiderable amount of water is drained from the clay as shown in Figure 8. For instance at the shutdown of the wells (10 years after the start of production) the cumulative water inflow is $15{\cdot}4 \times 10^6$ m^3 for the volumetric reservoir and $20{\cdot}5 \times 10^6$ m^3 for the waterdrive reservoir. In this case (reservoir permeability $k = 12{\cdot}8$ md) the quantity of water drained from the bounding clay is greater than the inflow from the adjacent aquifer. The difference between

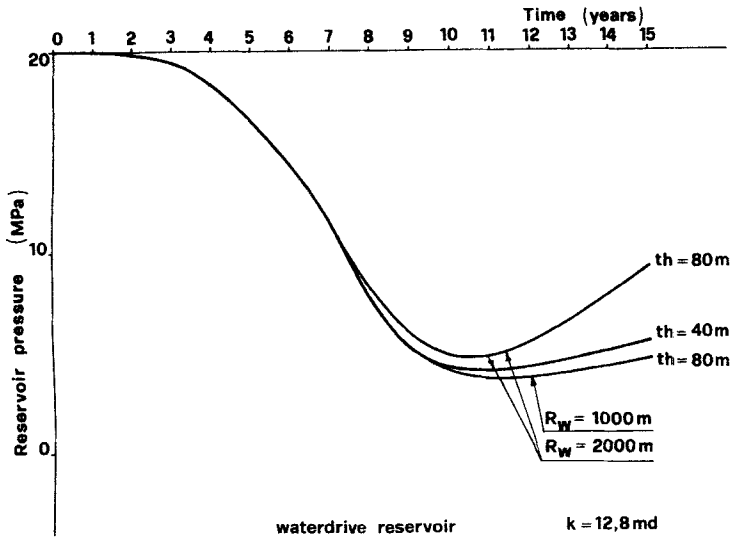

Figure 4. Waterdrive reservoir: effects of the reservoir radius and formation thickness on the reservoir pressure in time

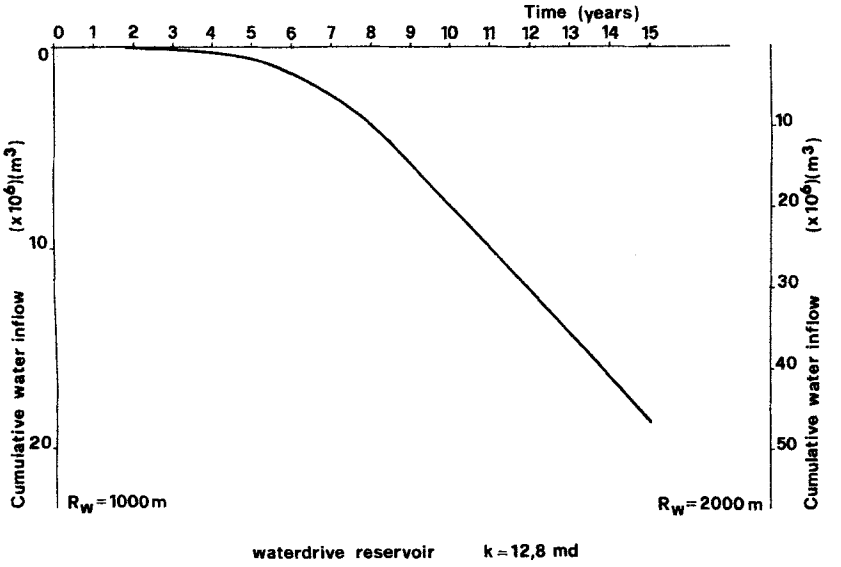

Figure 5. Waterdrive reservoir: water inflow versus time for two values of the reservoir radius

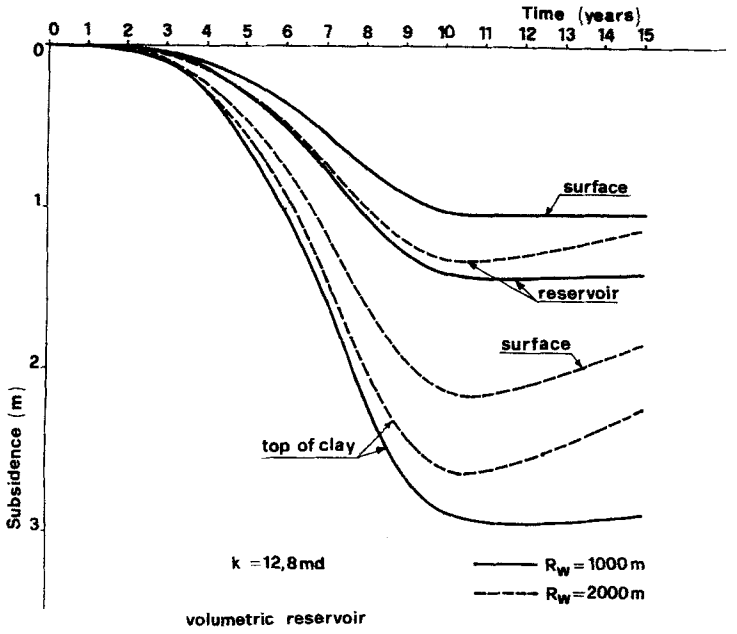

Figure 6. Volumetric reservoir: settlement in time for two values of the reservoir radius

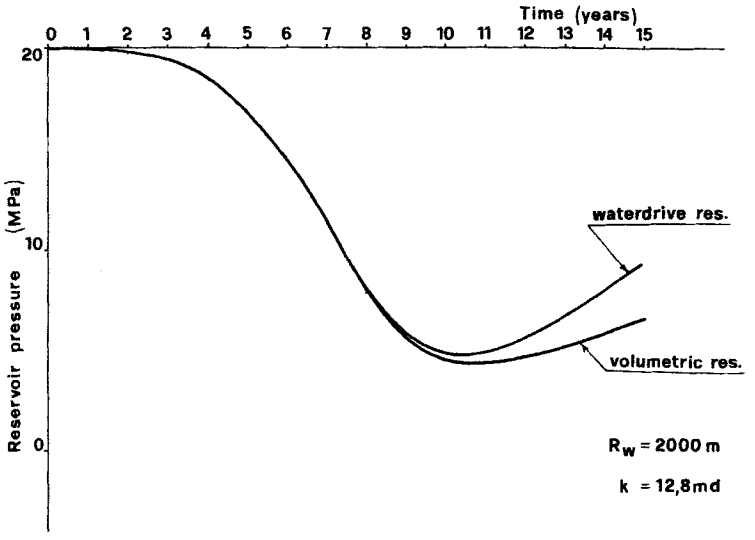

Figure 7. Reservoir pressure in time for a volumetric and a waterdrive gas reservoir

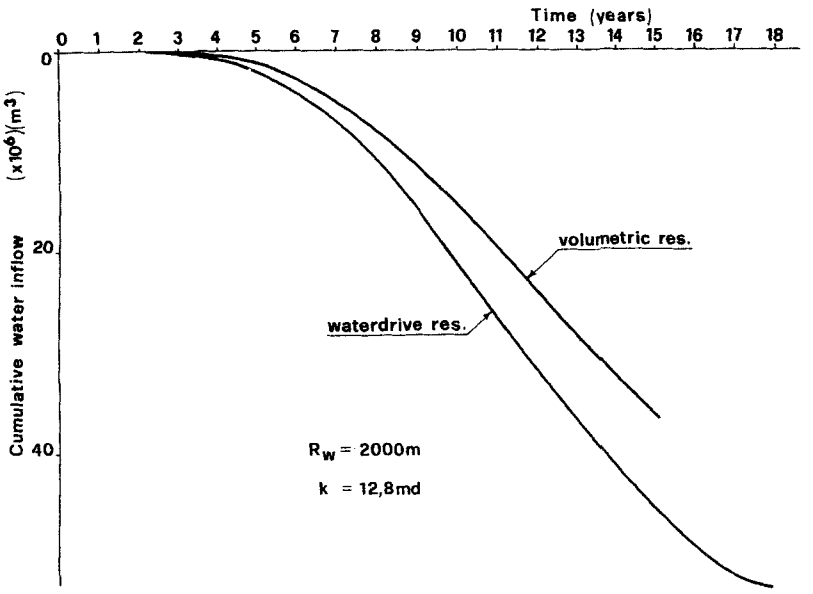

Figure 8. Cumulative water inflow in a waterdrive reservoir and a volumetric reservoir bounded by clay

these cumulative water inflows is increasing with the time, causing varying behaviour during recovery of the settlement. Similar conclusions can be made when comparing the diagrams for $R_w = 1000$ m of Figures 3 and 6. It is important to point out that the quantity of water drained from the surrounding clay is disregarded in the poroelasticity models. The enormous quantity of water drained from the clay compared to the encroaching edge water explains also the almost negligible difference between the maximum values of the reservoir pressure drop in the two reservoir types shown in Figure 7.

The reservoir pressure versus time and the cumulative water inflow for a volumetric reservoir with radius $R_w = 1000$ m and 2000 m are shown respectively in Figures 9 and 10. Again the recovery of the reservoir pressure for $R_w = 1000$ m is significantly smaller than for $R_w = 2000$ m. At 10 years from the beginning of the production the cumulative water inflow for $R_w = 2000$ m is 3·6 times that for $R_w = 1000$ m.

The subsidence bowl profiles at the closedown of the wells for a waterdrive and a volumetric reservoir are compared in Figure 11. Ninety per cent of the maximum subsidence is reached in the two cases respectively at a radial distance of 4250 m and 2900 m. The areal extent of the bowl is significantly larger for the waterdrive reservoir than for the volumetric reservoir. This is due to the fact that the lateral aquifer extends the influence zone of the pressure gradient and that the clay above the aquifer is also consolidating. This fact again is disregarded in the poroelasticity models. The subsidence bowl profiles, the settlement at the top of the clay layer and the reservoir compaction versus radial distance for both types of reservoir and for $R_w = 1000$ m are compared in Figure 12. The conclusions are the same as for the previous figure. In the case of the volumetric reservoir the effects of a large settlement distribution over a small area at the top of the clay layer are not completely transmitted to the ground surface.

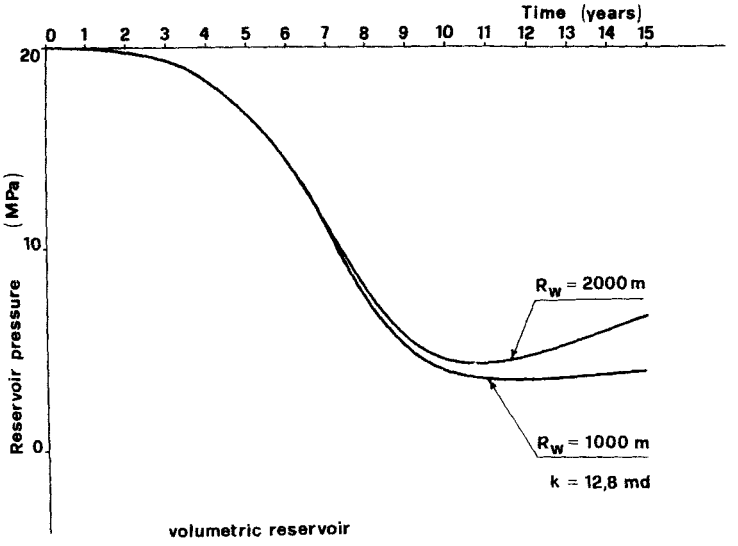

Figure 9. Volumetric reservoir: effects of the reservoir radius on the reservoir pressure in time

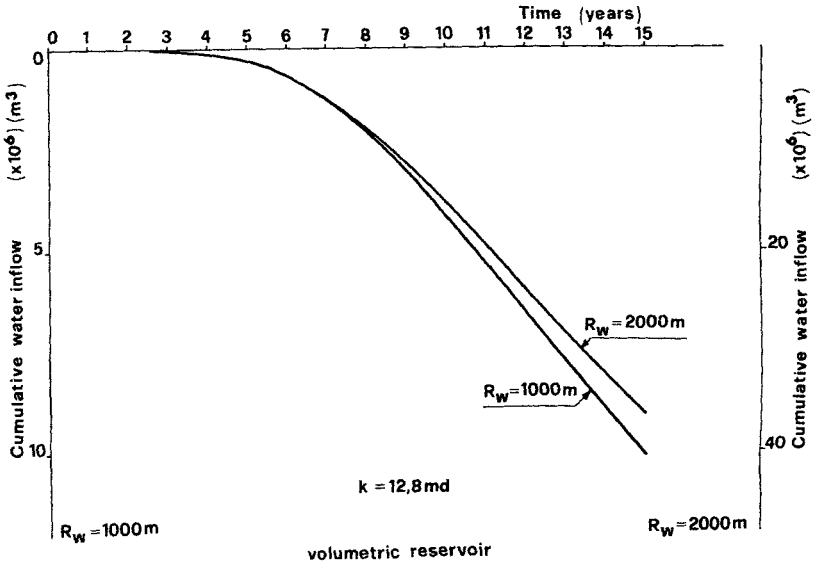

Figure 10. Volumetric reservoir: effects of the reservoir radius on the cumulative water inflow

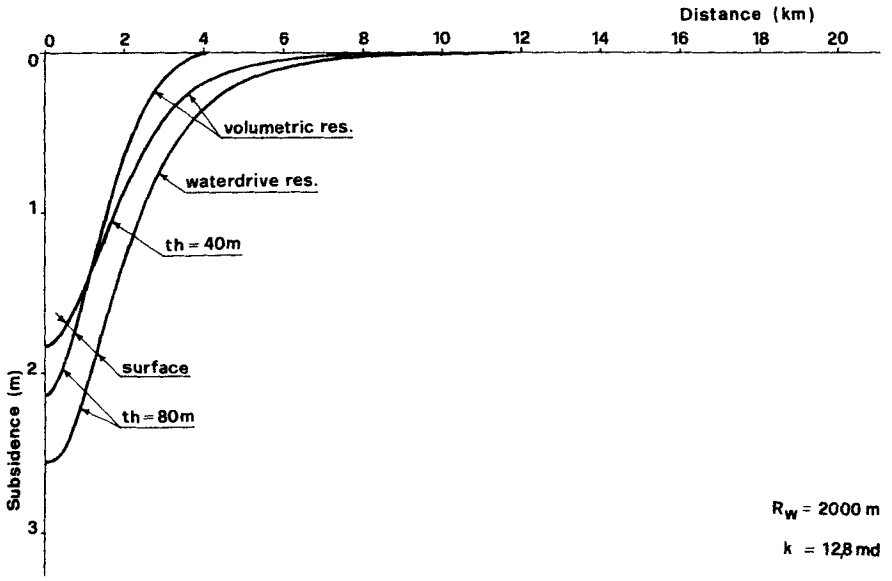

Figure 11. Subsidence bowl profile at the closedown of the wells above a volumetric and a waterdrive reservoir. Reservoir radius 2000 m

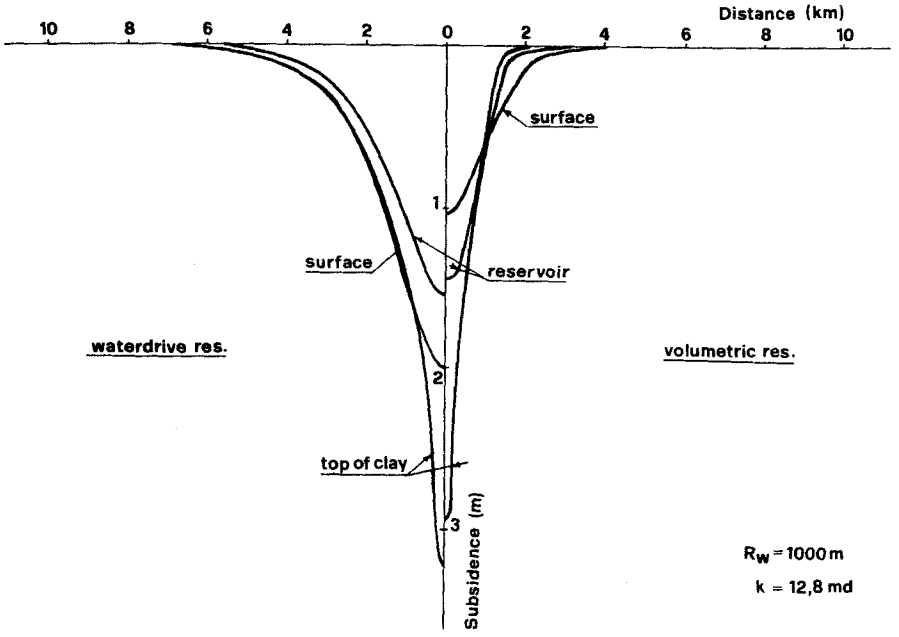

Figure 12. Subsidence bowl profile and settlements at different levels at the closedown of the wells for a volumetric and a waterdrive reservoir; reservoir radius 1000 m

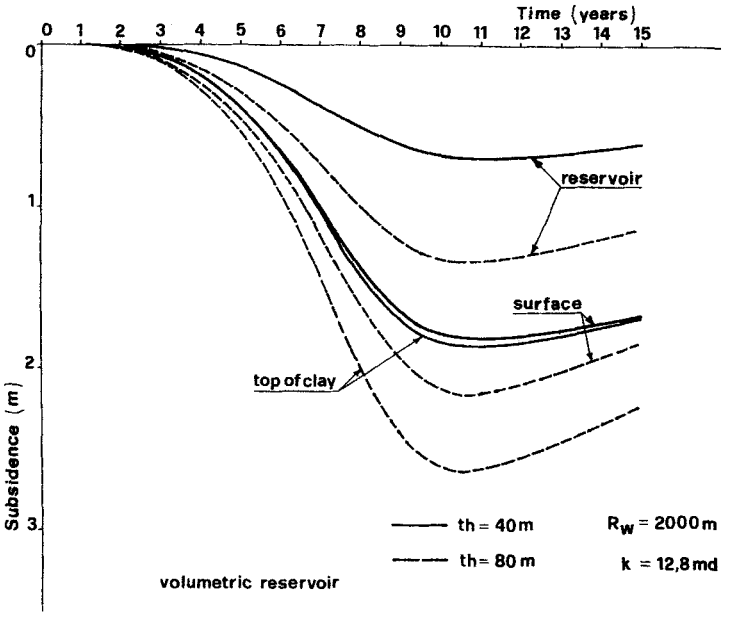

Figure 13. Volumetric reservoir: effects of the formation thickness on the settlement versus time

Finally the effects of the formation thickness on the surface subsidence have been investigated. The settlement versus time at the centre of the reservoir is compared (Figure 13) between two volumetric reservoirs with thicknesses of 80 m and 40 m, respectively. The maximum reservoir compaction in the second case is about the half of that in the first case. The surface subsidence increases but less in percentage terms than the formation thickness. The effects of the formation thickness upon the water inflow in a waterdrive reservoir are shown in Figure 14. For instance at 10 years the cumulative water inflow for a reservoir thickness of 80 m is 1·58 times that of a similar reservoir with a thickness of 40 m.

Further investigations regarding the influence of the depth of burial on the surface subsidence have shown that the reservoir compaction is not affected while the surface subsidence is increasing with decreasing depth of burial. These findings are in accordance with those obtained in Reference 5.

CONCLUSIONS

The following conclusions can be derived from parametric investigations regarding the ground subsidence above volumetric and waterdrive gas reservoirs, made with a fully coupled consolidation model.

The existence of clay layers bounding an exploited reservoir can influence substantially the surface subsidence.

The diameter of a subsidence bowl above a waterdive reservoir is considerably larger than above a similar volumetric reservoir.

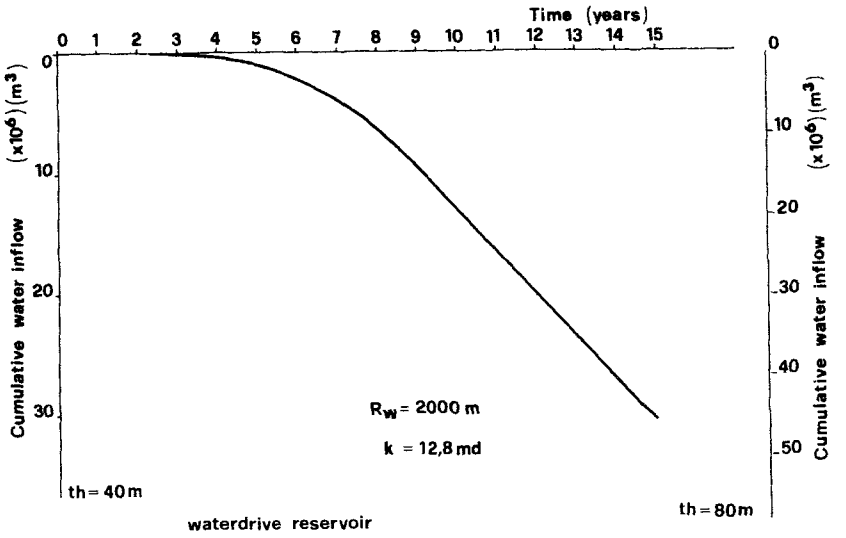

Figure 14. Waterdrive reservoir: effects of the formation thickness on the cumulative water inflow

The quantity of water drained from bounding clay layers can become significant and produce a waterdrive effect in volumetric reservoirs.

In similar situations a fully coupled consolidation model simulates the real subsidence behaviour more realistically than a poroelasticity model.

ACKNOWLEDGEMENTS

The research reported here received support from the National Research Council (Italy) under grant 78.02657.07.

The authors are also grateful for the computing facilities of the University College of Swansea, where most of the calculations were made.

REFERENCES

1. J. Geertsma, 'Land subsidence above compacting oil and gas reservoirs', *J. Petroleum Technology*, 734–744, June (1973).
2. J. Geertsma, 'Problems of rock mechanics in petroleum production engineering', *Proc. 1st Conf. Int. Soc. Rock Mech.*, **1**, 585–594, Lisbon (1966).
3. B. A. Schrefler and R. W. Lewis, 'A consolidation analysis of a waterdrive gas reservoir', *Proc. 3rd Int. Conf. Finite Elements in Flow Problems*, Banff (1980).
4. G. Evangelisti and B. Poggi, 'Sopra i fenomeni di deformazione dei terreni da variazione della pressione di strato', *Memorie, Serie II*, Atti della Accademia delle Scienze dello Istituto di Bologna (1970), No. 6.
5. A. Finol and S. M. Farouq Ali, 'Numerical simulation of oil production with simultaneous ground subsidence', *S.P.E. J.* **15**, 411–424 (1975).
6. R. W. Lewis and B. A. Schrefler, 'A fully coupled consolidation model of the subsidence of Venice', *Water Res. Res.*, **14**, 223–230 (1978).
7. B. A. Schrefler, R. W. Lewis and V. A. Norris, 'A case study of the surface subsidence of the Polesine area', *Int. J. Numer. Anal. Methods Geomech.* **1**, 377–386 (1977).
8. D. Schiavini (Ed.), 'L'abbassamento del suolo della zonq litoranea Ravennate', *Consorzio di Bonifica di Ravenna*, Ravenna (1976).

9. R. W. Lewis, I. R. White and K. Morgan, 'The influence of fluid withdrawal from underground reservoirs on surface settlement beneath offshore structures', To be published.
10. B. C. Craft and M. F. Hawkins, 'Applied petroleum reservoir engineering', Prentice Hall, Englewood Cliffs, N.J., 1959.
11. J. M. Duncan and C.-Y. Chang, 'Non-linear analysis of stress and strain in soils', *J. Soil Mech. Found. Div., ASCE*, Sept. (1970).